

Non-Equilibrium Dynamics of a Dissipative Two-Site Hubbard Model Simulated on the IBM Quantum Computer

Sabine Tornow

*Department of Computer Science and Mathematics,
Munich University of Applied Sciences, Lothstrasse 64, D-80335 Munich, Germany*

Wolfgang Gehrke and Udo Helmbrecht

Research Institute CODE, Universität der Bundeswehr München, Carl-Wery-Str. 22, D-81739 Munich

(Dated: December 22, 2024)

Many-body physics is one very well suited field for testing quantum algorithms and for finding working heuristics on present quantum computers. We have investigated the non-equilibrium dynamics of one- and two-electron systems, which are coupled to an environment that introduces decoherence and dissipation. In our approach, the electronic system is represented in the framework of a two-site Hubbard model while the environment is modelled by a spin bath. In order to simulate the non-equilibrium population probabilities of the different states on the quantum computer we have encoded the electronic states and environmental degrees of freedom into qubits and ancilla qubits (bath), respectively. The total evolution time was divided into short time intervals, during which the system evolves. After each of these time steps, the system interacts with ancilla qubits representing the bath in thermal equilibrium. We have specifically studied spin baths leading to both, unital and non-unital dynamics of the electronic system and have found that electron correlations clearly enhance the electron transfer rates in the latter case. For short time periods, the simulation on the quantum computer is found to be in good qualitative agreement with the exact results. We also show that slight improvements are already possible with various error mitigation techniques while even significant improvements can be achieved by using the recently implemented single-qubit reset operations. Our method can be well extended to simulate electronic systems in correlated spin baths as well as in bosonic and fermionic baths.

I. INTRODUCTION

Recent remarkable technological advances of small quantum computing devices have led to the possibility of testing quantum computing paradigms and finding novel working heuristics. One of the most promising early applications of quantum computers has been the modeling of quantum chemistry systems with many degrees of freedom. [1–4] Available noisy intermediate-scale quantum (NISQ) devices however are still lacking error correction and fault tolerant operations. [5] Nevertheless, exploring in particular the non-equilibrium quantum dynamics of certain open many-body systems has been suggested as a useful near-term application of NISQ devices. The environment may be taken into account by modeling only those of its aspects which would directly affect the system. [6] Eventually, the entire environment may be modeled with only one ancilla qubit or even without any ancillas at all, but by utilising the intrinsic noise of the quantum computer itself. [6, 7]

Understanding the dynamics of open many-body systems is important in various fields of fundamental research, including, e.g., unrevealing the microscopic mechanism of electron transfer, proton-coupled electron transfer and energy transfer. These key processes in chemistry and biology, with natural energy storage or photosynthesis as prominent examples, feature remarkable energy conversion efficiencies. Advances in understanding such processes directly helps engineering important applications such as artificial energy storage and artificial photosyn-

thesis. [8–12]

To simulate the irreversible transfer inherent to these systems any realistic model needs to include vibronic degrees of freedom, e.g., the solvent, the protein or electromagnetic fluctuations leading to dissipation and decoherence. In this regard, a paradigmatic model is the spin-boson model [13] or its extended versions.

A minimal model, which includes both, electronic correlations and the coupling to an environment introducing dissipation and decoherence, is the two-site dissipative Hubbard model. It has been investigated with the help of real-time path integral Monte Carlo techniques [14] and the time-dependent numerical renormalization group. [15] The main findings were a quantum phase transition, a non-Boltzmann steady state due to a decoherence-free subspace as well as conditions for pair vs. sequential electron transfer.

Our aim is exploring possibilities to simulate the dissipative Hubbard model on an available quantum computer. Although different algorithms for the unitary dynamics of many particle systems modeled by a Hubbard model have been studied and benchmarked before [16–19], there are only a few reports [20–24] for quantum algorithms to simulate the inherent, non-unitary dynamics of dissipative systems. In Ref. [25], an investigation of the dynamics of an open quantum system was reported. A two-state system without inter-state hopping coupled to a spin bath was considered. Input parameters of the described algorithm were the system environment interaction, the spectral density of the environment as well as the temperature. The environment was represented by ancilla qubits

designed to have the same effect as the environment in the Hamiltonian. Ref. [23] reports the time evolution of the density matrix, simulated in the operator-sum representation with Kraus operators for the amplitude damping channel. The Kraus operators were converted to a unitary time evolution problem with the help of the Sz.-Nagy dilation theorem. Ref. [20] discusses a quantum algorithm for many fundamental open quantum systems with unital and non-unital, as well as Markovian and non-Markovian, dynamics. The authors showed that the IBM quantum computer is a robust testbed for implementing a number of theoretical open quantum systems.

Energy transfer has been experimentally simulated using NMR quantum computers. [26] For this purpose, the photosynthetic system was mapped to the NMR system and the effect of the environment was effectively mimicked by a set of pulses, which acted as a classical, pure dephasing noise. Recently, electron and energy transfer have been calculated on a quantum computer. [27] In that work, the unitary part of the transfer was calculated on the quantum computer while the dephasing was simulated on a classical computer.

In our work we simulate open many-body systems using the IBM quantum computer and have explicitly set out to simulate also the environment on the quantum computer. We have considered an open quantum many-body system where the system is described by a two-site Hubbard model. The Hubbard model is mapped onto qubits by a Jordan-Wigner transformation for a filling of one and two electrons. The time is discretized and a Trotter-Suzuki decomposition is used to calculate the time evolution of the system. The population probabilities are calculated and measured for the total time $t = n\Delta t$, where Δt is the discrete time step and n is the number of gate sequences determining the time evolution of the system and the system-bath interaction.

Our model can be mapped to a coupled two-spin system interacting with a spin bath, which has been calculated on a classical computer for 32 bath spins. [28] In our work the effective two-spin system is investigated for different couplings to the spin bath which is considered to be in thermal equilibrium, non-interacting and represented by a single ancilla qubit as proposed in Ref. [25]. The XY coupling to the bath state leads to an amplitude damping and a non-unital dynamics, whereas the ZZ coupling to the bath state leads to a phase damping and a unital dynamics.

We have also applied post-processing to mitigate the errors. For short times, the results on the quantum computer are found to be in good agreement with the exact results. Hence, the IBM quantum computer is a good platform for testing open quantum systems, and - more generally - for performing tests of, and experiments on, novel algorithm implementations and heuristics.

The paper is organized as follows: Sec. II is devoted to describing our model of the open quantum many-body system and the mapping on qubits and gates. In Sec. III, we describe the performed experiments on the IBM quan-

tum computer and compare the results with the exact theoretical values, finally briefly evaluating different error mitigation techniques. We summarize our results in Sec. IV and propose work for future studies.

II. MODEL AND METHODS

In the following, we will describe our simulation of the dynamics of an open quantum system on the IBM quantum computer, which is represented by the Hamiltonian

$$H = H_{\text{sys}} \otimes \mathbb{I}_{\text{bath}} + \mathbb{I}_{\text{sys}} \otimes H_{\text{bath}} + H_{\text{sys-bath}}. \quad (1)$$

where H_{sys} , H_{bath} and $H_{\text{sys-bath}}$ are, respectively, the system, bath and interaction Hamiltonians, and \mathbb{I} is the identity operator.

While it is more common to consider a bath of harmonic oscillators, [15] we choose here instead a spin bath for the quantum computer. This spin bath is fully characterized by the spectral function $J(\omega)$, depending on the distribution of frequencies ω and couplings. The influence of the system on the environment is neglected.

It was shown in Ref. [25] that a large environment can be simulated by resetting the bath into its thermal equilibrium state during the calculation. The spectral density $J(\omega)$ is discretized in different modes, each of which is represented by a single qubit. In general, already a single ancilla qubit could be sufficient to represent the entire environment. We consider the two-site Hubbard model filled with one or two electrons coupled to an environment or bath, as depicted in Fig. 1 (upper panel). We assume that the system and bath are initially in a product state of density matrices $\rho_{\text{System}} \otimes \rho_{\text{bath}}$. Since we are only interested in the dynamics of the electronic system, we partially trace out the bath degrees of freedom leading to the completely positive map

$$\rho \rightarrow \text{Tr}_{\text{bath}} (U(\rho_{\text{system}} \otimes \rho_{\text{bath}})U^\dagger) \quad (2)$$

which describes the density matrix of the electronic system at t , and $U = e^{-iHt}$ is the unitary time evolution operator imposed on the total electron-bath system. The density matrix ρ_{bath} is forced back into the thermal equilibrium after the interaction with the system. Alternatively, a fresh qubit can be chosen.

To set up the full model, we need one or two system qubits s and bath qubits b_1 to b_d (see Fig. 1, lower panel). The time evolution in the Trotter form is implemented by the operator $U(\Delta t) = \mathcal{N}(\Delta t)\mathcal{U}(\Delta t)$, where $\mathcal{U}(\Delta t)$ implements the time evolution of the system and $\mathcal{N}(\Delta t)$ describes the interaction with the bath qubits, representing the bath in thermal equilibrium. This procedure is repeated n times and the occupation probability is measured during the time $t = n \cdot \Delta t$. After each interaction with the bath its degrees of freedom are traced out since they do not affect the electronic system (system qubits). This is very similar to the collision approach

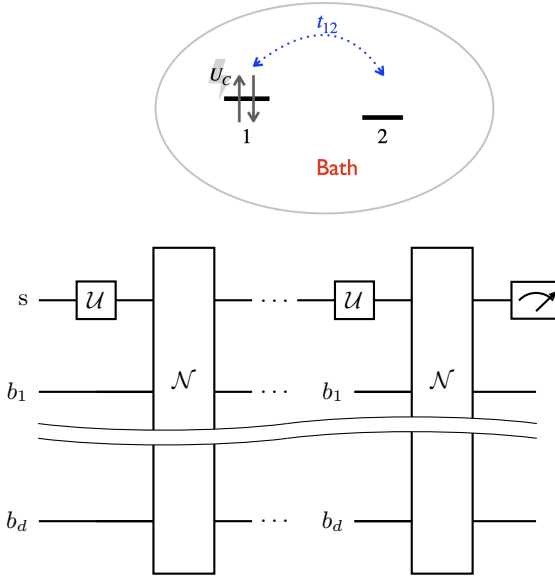


Figure 1. Upper panel: Pictorial representation of the Hubbard model with two sites coupled to the bath (environment). Site 1 is occupied with two electrons. The blue dotted arrow indicates the single-electron hopping matrix element t_{12} between the two sites. The on-site repulsion energy of two electrons on the same site is U_C . Lower panel: Schematic implementation of trotterized evolution of the open quantum system under study. The system comprises the electronic system qubits s and the bath qubits b_1 to b_d , which represent the d bath modes of the bath in thermal equilibrium. The time evolution is implemented by a Trotter step, the operator $U \approx \mathcal{N}U$, where U implements the time evolution of the system and \mathcal{N} describes the interaction with the bath qubits which were reset after each step. The reduced state of the electronic system alone is obtained by the indicated measurement.

where decoherence and dissipation are introduced by repeated collisions between system and bath qubits during a time interval Δt . [20, 29] In the following chapter we will first discuss the electronic system.

A. Electronic System

In the electronic system we consider a two-site Hubbard model (Fig 1)

$$H_{\text{sys}} = \sum_{\sigma, i=1,2} \varepsilon_i c_{i,\sigma}^\dagger c_{i,\sigma} + t_{12} \sum_{\sigma} (c_{2,\sigma}^\dagger c_{1,\sigma} + c_{1,\sigma}^\dagger c_{2,\sigma}) + U_C \sum_{i=1,2} c_{i\uparrow}^\dagger c_{i\uparrow} c_{i\downarrow}^\dagger c_{i\downarrow} \quad (3)$$

where $c_i(c_i^\dagger)$ denotes a fermionic annihilation (creation) operator for electrons on site $i = 1, 2$ with spin σ . ε_i is the onsite energy, t_{12} depicts the hopping matrix element between the two sites and U_C is the onsite Coulomb

repulsion.

The Hilbert space can be divided in different subspaces. With a filling of one electron we effectively deal with a two-state system with $|0\rangle = |\uparrow, 0\rangle$ and $|1\rangle = |0, \uparrow\rangle$. The subsystem with two electrons and its total spin equal to zero is spanned by the states $|0\rangle = |\uparrow\downarrow, 0\rangle$, $|1\rangle = |\downarrow, \uparrow\rangle$, $|2\rangle = |\uparrow, \downarrow\rangle$ and $|3\rangle = |0, \uparrow\downarrow\rangle$ with the notation $|\text{site1}, \text{site2}\rangle$ describing the occupation on site 1 and site 2, respectively. We discuss both subspaces in more detail in the following.

1. Filling with one electron

In the subspace with one electron, which is spanned by $|0\rangle$ and $|1\rangle$, we can rewrite the Hamiltonian

$$H_{\text{sys}} = \varepsilon \sigma_z + t_{12} \sigma_x, \quad (4)$$

with $\varepsilon_1 = -\varepsilon$, $\varepsilon_2 = \varepsilon$, and σ_x , σ_z are the Pauli matrices. To simulate the time evolution of the population probabilities we discretize the time $t = n \cdot \Delta t$ and write the time evolution operator as

$$e^{-iHt} = (e^{-iH\Delta t})^n \quad (5)$$

and trotterize the Hamiltonian of the electronic system into the non-commuting parts $\varepsilon \cdot \sigma_z$ and $t_{12} \cdot \sigma_x$

$$U(t) = e^{-iH_{\text{sys}}t} \approx (e^{-it_{12} \cdot \sigma_x \cdot \Delta t} e^{-i\epsilon \cdot \sigma_z \cdot \Delta t})^n. \quad (6)$$

The circuit of one time step is shown in Fig. 2 (a) with

$$R_x(2 \cdot t_{12} \cdot \Delta t) = e^{-it_{12} \cdot \sigma_x \cdot \Delta t} = \begin{pmatrix} \cos(t_{12} \cdot \Delta t) & -i \sin(t_{12} \cdot \Delta t) \\ -i \sin(t_{12} \cdot \Delta t) & \cos(t_{12} \cdot \Delta t) \end{pmatrix} \quad (7)$$

and

$$R_z(2 \cdot \epsilon \cdot \Delta t) = e^{-i\epsilon \cdot \sigma_z \cdot \Delta t} = \begin{pmatrix} e^{-i\epsilon \cdot \Delta t} & 0 \\ 0 & e^{i\epsilon \cdot \Delta t} \end{pmatrix} \quad (8)$$

We can approximate the time evolution operator for small Δt :

$$U(n \cdot \Delta t) \approx (R_x(2 \cdot t_{12} \cdot \Delta t) \cdot R_z(2 \cdot \epsilon \cdot \Delta t))^n \quad (9)$$

and implement it on the quantum computer for the circuit in Fig. 2 (a).

2. Filling with two electrons

In the subspace with two electrons which is spanned by $|0\rangle$, $|1\rangle$, $|2\rangle$ and $|3\rangle$ we can rewrite the Hamiltonian in the Pauli matrix form

$$H = H_t + H_U \quad (10)$$

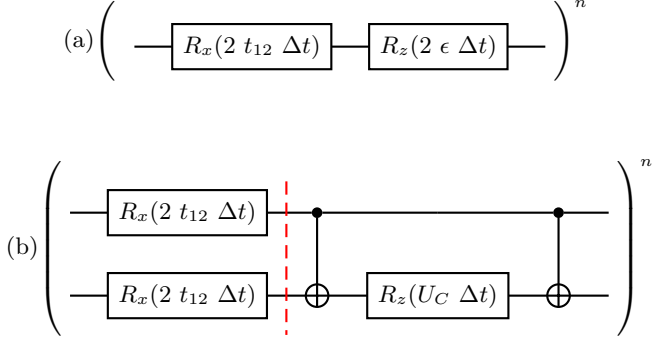


Figure 2. Circuit implementation of the single-electron time evolution with discrete evolution operators $R_x(2 t_{12} \cdot \Delta t)R_z(2 \epsilon \cdot \Delta t)$ (circuit (a)) and the two-electron time evolution split into the kinetic part $R_x(2 t_{12} \cdot \Delta t) \otimes R_x(2 t_{12} \cdot \Delta t)$ before the dashed line and the Coulomb interaction part $R_{ZZ}(U_C \cdot \Delta t)$, eq. (17), after the dashed line (circuit (b)). The gate sequence is repeated n times for the time $t = n\Delta t$.

with

$$H_t = t_{12} (\mathbb{I}_2 \otimes \sigma_x + \sigma_x \otimes \mathbb{I}_2) \quad (11)$$

and

$$H_U = \frac{U_c}{2} (\sigma_z \otimes \sigma_z) \quad (12)$$

with $\epsilon = 0$.

We discretize the time $t = n \cdot \Delta t$. The time evolution operator is approximately decomposed (Trotter-Suzuki) in the product form

$$U(t) \approx (e^{-iH_t\Delta t} \cdot e^{-iH_C\Delta t})^n \quad (13)$$

with

$$e^{-iH_t\Delta t} = e^{-it_{12}\cdot\sigma_x\Delta t} \otimes e^{-it_{12}\cdot\sigma_x\Delta t} \quad (14)$$

$$= R_x(2 \cdot t_{12} \cdot \Delta t) \otimes R_x(2 \cdot t_{12} \cdot \Delta t) \quad (15)$$

The second factor of Eq. (13) can be written as:

$$e^{-iH_C\Delta t} = e^{-i\frac{U_c}{2}(\sigma_z \otimes \sigma_z)\Delta t} \quad (16)$$

$$= \begin{pmatrix} e^{-i\frac{U_c\Delta t}{2}} & 0 & 0 & 0 \\ 0 & e^{i\frac{U_c\Delta t}{2}} & 0 & 0 \\ 0 & 0 & e^{i\frac{U_c\Delta t}{2}} & 0 \\ 0 & 0 & 0 & e^{-i\frac{U_c\Delta t}{2}} \end{pmatrix}$$

which is $U_{\text{CNOT}}(\mathbb{I}_2 \otimes R_z(U_c \cdot \Delta t))U_{\text{CNOT}} = R_{ZZ}(U_c \cdot \Delta t)$. The gates for the unitary time evolution operator

$$U(n \cdot \Delta t) \approx ((R_x(2 \cdot t_{12} \cdot \Delta t))^{\otimes 2} R_{ZZ}(U_c \cdot \Delta t))^n \quad (17)$$

are displayed in Fig. 2 (b). In the next section we discuss the bath and the coupling to the bath.

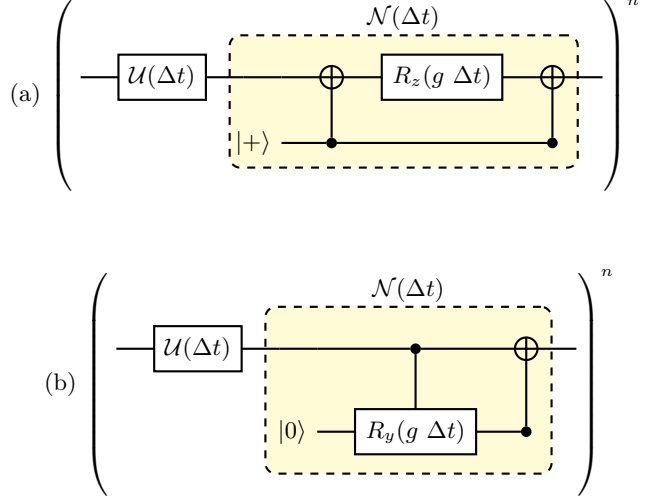


Figure 3. Circuit implementation of the single-electron bath time evolution $U(\Delta t) = \mathcal{N}(\Delta t)\mathcal{U}(\Delta t)$ with discrete evolution operator $\mathcal{U}(\Delta t)$ followed by the interaction with the bath $\mathcal{N}(\Delta t)$. Circuit (a) leads to phase damping and circuit (b) to amplitude damping, respectively. The circuit for the two-electron time evolution (not shown) is similar, but each qubit line is coupled to the bath qubit via $\mathcal{N}(\Delta t)$.

B. Environment

For the environment we consider a bath of independent two-level systems (spins) in thermal equilibrium. Here, we are showing the coupling to the single-electron subspace. The coupling to the system for the two-electron subspace is done similarly. We consider two different models for the bath and its coupling to the system, first, for the ZZ coupling

$$H_{\text{sys-bath}}^{\text{ZZ}} = \sum_{k=1}^d g_k (\sigma_z \otimes \sigma_{z,k}) \quad (18)$$

$$H_{\text{bath}}^{\text{ZZ}} = - \sum_{k=1}^d \omega_k \sigma_{x,k} \quad (19)$$

and second, the XY coupling

$$H_{\text{sys-bath}}^{\text{XY}} = \sum_{k=1}^d g_k (\sigma_x \otimes \sigma_{x,k} + \sigma_y \otimes \sigma_{y,k}) \quad (20)$$

$$H_{\text{bath}}^{\text{XY}} = - \sum_{k=1}^d \omega_k \sigma_{z,k} \quad (21)$$

where ω_k are the frequencies of the environment mode, g_k is the coupling coefficient for the k^{th} mode and d is the number of the bath modes.

We describe the electron dynamics by the reduced density matrix

$$\rho(t) \rightarrow \text{Tr}_{\text{bath}} (U (\rho_{\text{system}} \otimes \rho_{\text{bath}}) U^\dagger) \quad (22)$$

We assume that the initial density matrix is a tensor product of the system and the bath density matrices and

that the bath degrees of freedom are in their thermal equilibrium. We discretize the time in $t = n\Delta t$ and at every time step we apply the unitary time evolution operator

$$U(\Delta t) = \mathcal{N}(\Delta t)\mathcal{U}(\Delta t) \quad (23)$$

During the time interval Δt the electronic system interacts locally with the degrees of freedom of the environment, i.e., the ancilla qubits as shown in Fig. 1 (lower panel). For the population probability at time t we need $n \cdot d$ ancilla qubits. Here we use the approximation that the whole bath is represented by one qubit, so that we have to reset the qubit n times or use n fresh qubits in the single electron case. We are only interested in the degrees of freedom of the electronic system and calculate the reduced density operator:

$$\rho(n) \rightarrow \text{Tr}_{\text{bath}}((\mathcal{N}\mathcal{U})^n(\rho_{\text{System}} \otimes \rho_{\text{bath}})(\mathcal{U}^\dagger \mathcal{N}^\dagger)^n)$$

The electronic system evolves for the time Δt with the unitary time evolution

$$\mathcal{U} = e^{-iH_{\text{sys}}\Delta t} \quad (24)$$

and interacts with one of the ancilla qubits which represent the entire bath. The unitary time evolution is

$$\mathcal{N}^{ZZ} = e^{-ig(\sigma_z \otimes \sigma_z)\Delta t} \quad (25)$$

The bath qubit is in thermal equilibrium which can be emulated in this case by putting each of the n bath qubits into the state $\rho_{\text{bath}} = |+\rangle\langle +|$.

The operator \mathcal{N}^{ZZ} acts as follows:

$$\mathcal{N}^{ZZ}(|0\rangle_{\text{sys}} \otimes |0\rangle_{\text{bath}}) = e^{-\frac{ig\Delta t}{2}}(|0\rangle_{\text{sys}} \otimes |0\rangle_{\text{bath}}) \quad (26)$$

$$\mathcal{N}^{ZZ}(|0\rangle_{\text{sys}} \otimes |1\rangle_{\text{bath}}) = e^{-\frac{ig\Delta t}{2}}(|0\rangle_{\text{sys}} \otimes |1\rangle_{\text{bath}}) \quad (27)$$

$$\mathcal{N}^{ZZ}(|1\rangle_{\text{sys}} \otimes |0\rangle_{\text{bath}}) = e^{-\frac{ig\Delta t}{2}}(|1\rangle_{\text{sys}} \otimes |0\rangle_{\text{bath}}) \quad (28)$$

$$\mathcal{N}^{ZZ}(|1\rangle_{\text{sys}} \otimes |1\rangle_{\text{bath}}) = e^{\frac{ig\Delta t}{2}}(|1\rangle_{\text{sys}} \otimes |1\rangle_{\text{bath}}) \quad (29)$$

The bath is simulated with the circuits depicted in Fig. 3. After the collision, the electronic system evolves with $\mathcal{U}(\Delta t)$. Then the system interacts with the next ancilla qubit in the initial state $|+\rangle$. The electronic system is measured at $t = n\Delta t$ after n collisions (n repetitions of the circuit). The successive collisions introduce a phase damping $\rho \rightarrow \frac{1}{2}\mathbb{I}_2$ or $\rho \rightarrow \frac{1}{4}\mathbb{I}_4$.

For the second example (the XY interaction) the time evolution is given by

$$\mathcal{N}^{XY} = e^{-ig(\sigma_x \otimes \sigma_x + \sigma_y \otimes \sigma_y)\Delta t}. \quad (30)$$

For the XY coupling the operator acts as follows. (The bath qubits are in the thermal state $|0\rangle$.)

$$\mathcal{N}^{XY}(|0\rangle_{\text{sys}} \otimes |0\rangle_{\text{bath}}) = |0\rangle_{\text{sys}} \otimes |0\rangle_{\text{bath}} \quad (31)$$

$$\begin{aligned} \mathcal{N}^{XY}(|1\rangle_{\text{sys}} \otimes |0\rangle_{\text{bath}}) &= \sin(g\Delta t)(|0\rangle_{\text{sys}} \otimes |1\rangle_{\text{bath}}) \\ &\quad + \cos(g\Delta t)(|1\rangle_{\text{sys}} \otimes |0\rangle_{\text{bath}}) \end{aligned}$$

After each collision, the electronic system interacts with the next ancilla qubit in the state $\rho_{\text{bath}} = |0\rangle\langle 0|$. After multiple interactions, the process leads to amplitude damping and $|1\rangle \rightarrow |0\rangle$.

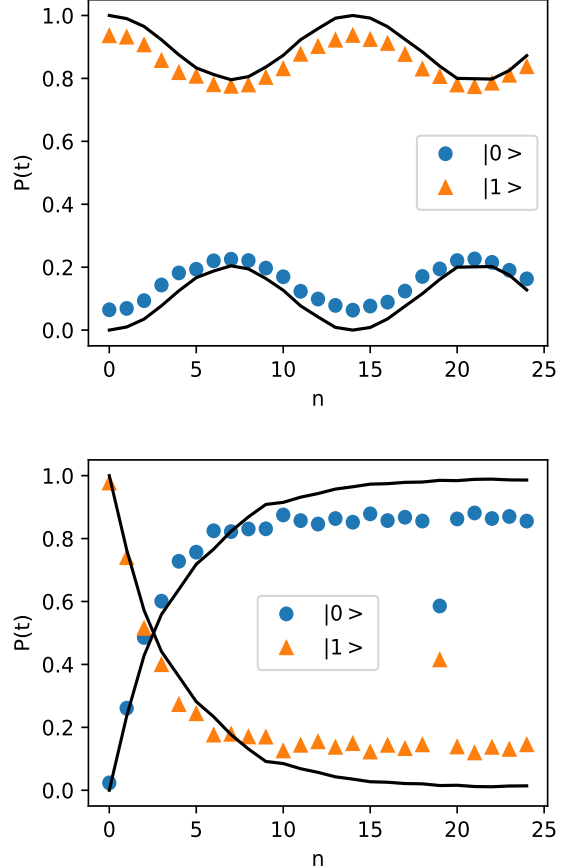


Figure 4. Upper panel: Population probabilities $P(t)$ as a function of the discrete time steps n , exact (black line) and simulated on the Manhattan quantum computer, of site 2 (blue circles) and site 1 (orange triangles) with $\epsilon \cdot \Delta t = 0.2$, $t_{12} \cdot \Delta t = 0.1$. Lower panel: Population probabilities with the same parameters but with a finite coupling $g \cdot \Delta t = 0.5$ to the spin bath (XY coupling), which leads to non-unital dynamics (amplitude damping).

III. QUANTUM SIMULATION OF THE NON-EQUILIBRIUM DYNAMICS

We have implemented the algorithms depicted in Figs. 2 and 3 for the two-site Hubbard model alone, and for the dissipative Hubbard model on the 27 and 65 qubits IBM Q devices *Paris*, *Toronto* and *Manhattan* and performed 8192 runs for each circuit. For the bath qubit, we used either n ancilla qubits in the initial state or we used the recently available reset option, which is performed n times for the single electron case and $2n$ times for the two-electron case if every system qubit is coupled to a different bath qubit. To trace out the bath, we measured the one or two system qubits at the end of the circuit sequence.

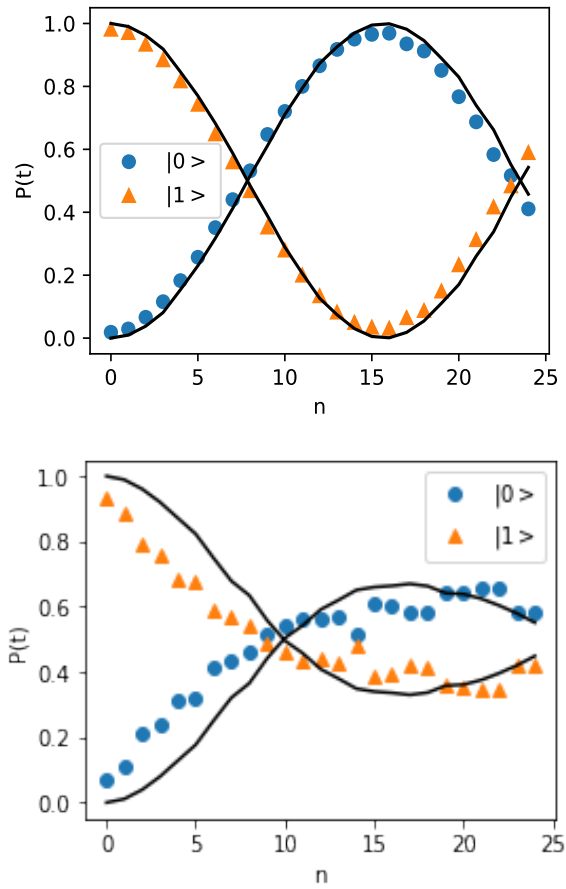


Figure 5. Upper panel: Population probabilities $P(t)$ as a function of the discrete time steps n , exact (black line) and simulated on the Manhattan quantum computer, of site 2 (blue circles) and site 1 (orange triangles) with $\epsilon \cdot \Delta t = 0$, $t_{12} \cdot \Delta t = 0.1$. Lower panel: Population probabilities with the same parameters but with a finite coupling $g \cdot \Delta t = 0.5$ to the spin bath (ZZ coupling), which leads to unital dynamics (phase damping).

1. Filling with one electron

We chose $n = 25$ and $\Delta t = 0.2$ so that the simulated, trotterized curve lies on the exact calculation. We measured the single electron population probabilities $n_1 = \text{Tr}(|0\rangle\langle 0| \rho(t))$ and $n_2 = \text{Tr}(|1\rangle\langle 1| \rho(t))$ with the initial condition $\rho_0 = |1\rangle\langle 1|$. The quantum circuit on the quantum computer is described in Fig. 2 (a). In Fig. 4 (upper panel) the well-known Rabi oscillations can be seen. The experimental result on the quantum computer coincides with the theoretical curve. [15]

For including the coupling to the bath we chose the XY coupling, which leads to amplitude damping, as simulated with the circuit shown in Fig. 3 (b). In Fig. 4 (lower panel) we start with $\rho_0 = |1\rangle\langle 1|$ for $t = 0$ and the bath qubits in state $|0\rangle$. The experimental curve is in very good agreement with the classical simulation. The amplitude damping introduced a decay of the state $|1\rangle$.

Counteracting to this decay is the hopping matrix element between the sites. The effective hopping for $\epsilon \gg t_{12}$ is t_{12}^2/ϵ , leading to a faster transfer in comparison to $\epsilon < t_{12}$.

For $\epsilon = 0$ the quantum computer reproduced the Rabi oscillations in (see, Fig. 5, upper panel) with damped oscillation when the bath featuring the ZZ coupling is coupled to the system. The deviation of experimental values, obtained by the bath qubit reset method, from the classical simulation appear to originate from the quantum computer itself, introducing an own amplitude damping component. Alternative to resetting the bath qubit n times we tried to use n different fresh bath qubits, which led to a faster thermalization already at $n = 5$ (not shown). This is due to multiple swapping operations which introduce noise. The computation shows that it is in principle possible to simulate open quantum one-electron systems on the quantum computer even without error mitigation, for short time scales.

2. Filling with two electrons

Second, we have simulated the population probabilities for the two electron subspace spanned by $|0,0\rangle, |0,1\rangle, |1,0\rangle, |1,1\rangle$. The probability that two electrons are occupying site 1 is $\text{Tr}(|0,0\rangle\langle 0,0| \rho(t))$ and for site 2 it is $\text{Tr}(|1,1\rangle\langle 1,1| \rho(t))$ (the two states with a single electron on each site are: $\text{Tr}(|0,1\rangle\langle 0,1| \rho(t))$ and $\text{Tr}(|1,0\rangle\langle 1,0| \rho(t))$) where $\rho(t) = \text{Tr}(U \rho_0 U^\dagger)$ with $U = e^{-iHt}$ and $t = n \cdot \Delta t$ which we simulated according to Eq. (17). The initial condition is "two electrons on site 2" ($\rho_0 = |1,1\rangle\langle 1,1|$). We first tested the Trotter approximation which was found to be in good agreement with the exact values until $n = 30$ (not shown). The experimental values on the *Manhattan* quantum computer obtained by including the post-processing error-mitigation scheme Ignis [30] agree qualitatively well (Fig 6 (upper panel)) to the theoretical values. The two-electron dynamics show pair oscillations: The electron pair oscillates between site 1 and 2 with the small frequency $\frac{4t_{12}^2}{U_C}$ whereas the fast oscillations with frequency U_C characterize the virtual population of the low lying states $|1,0\rangle$ and $|0,1\rangle$. [15] We will discuss different error mitigation schemes below. For the amplitude damping case in Fig. 6 (lower panel) the experimental values are lying on the exact simulation until $n = 5$. Then the values are approaching the equilibrium value, which deviates from the exact simulation. Here, due to the amplitude damping and small effective pair hopping t_{12}^2/U_C the initial state ($|1,1\rangle$) is decaying very fast towards the thermal equilibrium and two electrons are transferred to the other site irreversibly.

The experimental values for the ZZ coupling to the bath show a strong deviation from the exact simulation and are thermalizing much faster to the equilibrium value (not shown).

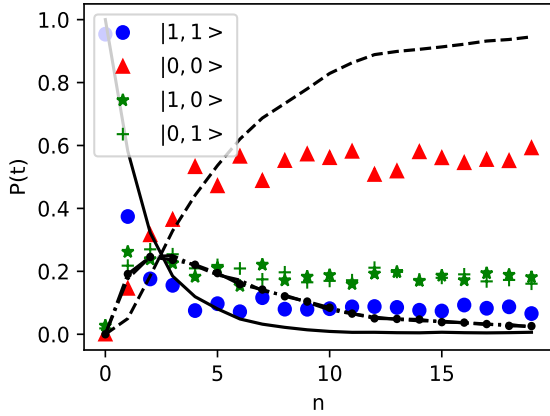
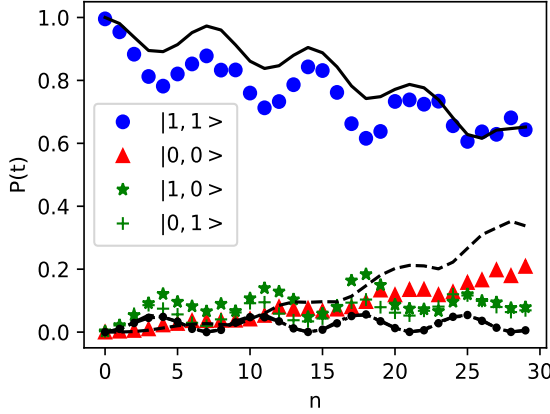


Figure 6. Upper panel: Experimental population probabilities $P(t)$ as a function of the number of time steps in comparison to the exact calculations (black line): doubly occupied site 2 (probability of $|1,1\rangle$, solid line), doubly occupied site 1, (probability of $|0,0\rangle$, dashed line) and the single occupied states (probability of $|0,1\rangle$ and $|1,0\rangle$, dot-dashed line). The parameters are $t_{12} \cdot \Delta t = 0.1$ and $U_C \cdot \Delta t = 0.4$. Starting point was two electrons on site 2. Lower panel: Population probabilities with the same parameters but with a finite coupling $g \cdot \Delta t = 0.5$ to the spin bath (XY coupling), which leads to non-unital dynamics (amplitude damping).

3. Error mitigation

Errors accumulate due to decoherence, dissipation as well as due to read-out errors. To evaluate the errors, we implemented the circuit shown in Fig. 2(b) but with the initial state being the entangled state $\frac{1}{\sqrt{2}}(|0,1\rangle - |1,0\rangle)$.

This state belongs to a decoherence-free subspace. Neither is the state changed by hopping nor by including decoherence if both electrons are coupled to the same bath. Therefore, the state has to remain unchanged for all n . In the experiment, only the $|0,1\rangle$ does not thermalize and stays constant. The circuit is symmetric with respect to the exchange of the qubit order. If we switch the order of the qubits, the other state $|1,0\rangle$ does not thermalize (not shown). Hence, we conclude that the error is introduced

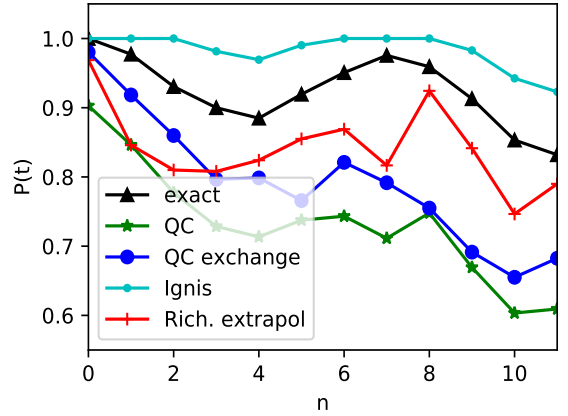
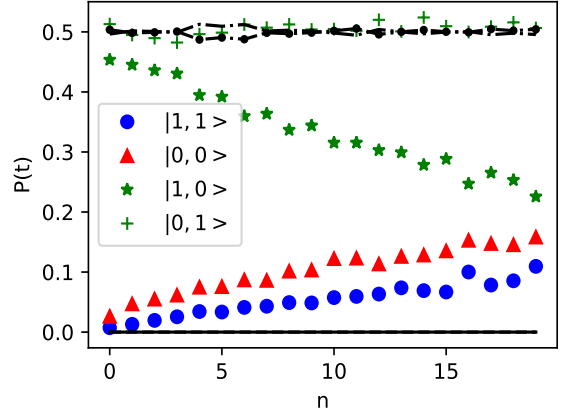


Figure 7. Upper panel: The same as upper panel of Fig. 6 but with initial state $\frac{1}{\sqrt{2}}(|0,1\rangle - |1,0\rangle)$. Lower panel: Comparison of different error mitigation methods for the occupation probability of state $|1,1\rangle$ as a function of the number of time steps n . The result on the *Manhattan* quantum computer (green stars) is improved by changing $|1\rangle$ to $|0\rangle$ (blue circles) and further improved by the zero noise Richardson extrapolation (red plus signs) in comparison to the exact values (black triangles). The ignis measurement calibration method (light blue dots) improves the result but overshoots the exact simulation.

only if the control qubit is $|1\rangle$, and therefore the error occurrence depends on the initial state.

We have tested bit flip error detection and post-selection of the erroneous values, but the overhead was too large and introduced too much noise itself. Therefore, we only present the error mitigation techniques here.

For the population probabilities in Fig. 6 (upper panel) we tested different error mitigation techniques for the probability of the state $|1,1\rangle$ in Fig. 7 for small n . To mitigate the error, the quantum circuit is thought of being composed of ideal gates, each of which accompanied by a noise channel similar to our model for the open quantum system $\mathcal{U} = \mathcal{N}\mathcal{U}$. We have systematically increased the circuit noise by doubling the number n of circuit parts and halving the time step Δt , and then we

extrapolated N to zero. With the additional measurements we were able to perform a Richardson extrapolation shown in Fig. 7 (red triangles with dashed line) which improved the result compared to the run on the quantum computer (green stars). The overall read-out noise can be effectively reduced with the Ignis technique (small dots) which was also used to generate the results shown in Fig. 6 (upper panel). The main errors stem from the CNOT gates and the decay of the $|1\rangle$ state during the calculation and measurement. An interchange of $|1\rangle$ and $|0\rangle$ improves the result (blue circles).

IV. CONCLUSION

We have studied quantum algorithm heuristics for simulating the time evolution of an open quantum system in an environment, which introduces decoherence and dissipation, on an IBM quantum computer. We simulated a two-site dissipative Hubbard model in the single and two-electron subspace, which were mapped onto one and two system qubits, respectively. This model is equivalent to an interacting two-spin system coupled to a non-interacting spin-bath, which is considered to be in thermal equilibrium.

We have discretized the time $t = n \cdot \Delta t$ and applied the Trotter-Suzuki approximation. The environment is modelled with n ($2n$) ancilla qubits or one ancilla qubit which was reset n ($2n$) times in the one (two-electron) case, respectively. Each ancilla qubit is representing the entire spin bath in thermal equilibrium. [25]

We considered two different couplings to bath qubits. The ZZ coupling leads to a phase damping whereas the XY coupling leads to amplitude damping, giving rise to non-unital dynamics of the system. As proposed in Refs. [20, 29, 31], we have implemented our system-bath interaction as "consecutive collisions" between system and bath qubits. The system evolves for the small time interval Δt during which it interacts with the bath in thermal equilibrium, with the strength g . After each time step n we trace out and disregard the bath degrees of freedom. We have started with simulating the system alone. The single electron Rabi oscillations are found to be quantitatively in very good agreement with the theoretical,

analytical result. The data of the two-electron dynamics show some deviations from the theoretical curve, but the agreement can be improved with error mitigation techniques. For large n equivalent to longer circuits the population probabilities thermalize and deviate strongly from the theoretical values. The main errors stem from the CNOT gates and the decay of the $|1\rangle$ state during the calculation and measurement. For small n , we have been able to improve the results by error mitigation, namely zero noise extrapolation as well as with the Ignis package. With the coupling to the bath decoherence and dissipation are introduced. The ZZ coupling to the spin-bath qubit, which leads to decoherence and unital phase damping, evokes damping of the Rabi oscillations and pair oscillation. The experimental data for the two-electron system show an earlier thermalization as predicted by the classical simulation. The XY coupling to the spin-bath qubit leads to dissipation and non-unital amplitude damping so that the system will irreversibly end up in state $|0\rangle$ or $|00\rangle$, respectively. Counteracting is the hopping matrix element which forces the system to go back to the other states. The effective hopping gets small for a large Coulomb interaction so that the dissipative environment in addition to the electronic correlations leads to a fast and irreversible electron-pair transfer.

In summary, we have demonstrated that today's emerging quantum computing hardware enables well the evaluation of heuristic quantum algorithms for open many-particle systems. To improve the experimental results, we plan to test other error mitigation schemes with hybrid techniques in future studies. We will investigate other environment models and couplings, e.g., ancilla qubits which simulate a bath of harmonic oscillators, a fermionic bath or correlated bath qubits to simulate non-Markovian processes.

ACKNOWLEDGMENTS

The results presented in this paper were obtained in part using an IBM Q quantum computing system as part of the IBM Q Network. The views expressed are those of the authors and do not reflect the official policy or position of IBM or the IBM Q team.

[1] S. McArdle, S. Endo, A. Aspuru-Guzik, S.C. Benjamin, and X. Yuan, "Quantum computational chemistry," *Reviews of Modern Physics* **92** (2020), 10.1103/RevModPhys.92.015003.

[2] Y. Cao, J. Romero, J.P. Olson, M. Degroote, P.D. Johnson, M. Kieferová, I.D. Kivlichan, T. Menke, B. Peropadre, N.P.D. Sawaya, S. Sim, L. Veis, and A. Aspuru-Guzik, "Quantum chemistry in the age of quantum computing," *Chemical Reviews* **119**, 10856–10915 (2019), cited By 15.

[3] Alexander J. McCaskey, Zachary P. Parks, Jacek Jakowski, Shirley V. Moore, Titus D. Morris, Travis S. Humble, and Raphael C. Pooser, "Quantum chemistry as a benchmark for near-term quantum computers," *npj Quantum Information* **5**, 99 (2019).

[4] Bela Bauer, Sergey Bravyi, Mario Motta, and Garnet Kin-Lic Chan, "Quantum algorithms for quantum chemistry and quantum materials science," (2020), [arXiv:2001.03685 \[quant-ph\]](https://arxiv.org/abs/2001.03685).

[5] John Preskill, "Quantum Computing in the NISQ era and beyond," *Quantum* **2**, 79 (2018).

[6] Seth Lloyd, “Universal quantum simulators,” *Science* **273**, 1073–1078 (1996).

[7] Brian Rost, Barbara Jones, Mariya Vyushkova, Aaila Ali, Charlotte Cullip, Alexander Vyushkov, and Jarek Nabrzyski, “Simulation of thermal relaxation in spin chemistry systems on a quantum computer using inherent qubit decoherence,” (2020), [arXiv:2001.00794 \[quant-ph\]](https://arxiv.org/abs/2001.00794).

[8] Rudolph A. Marcus, “Electron transfer reactions in chemistry: Theory and experiment (nobel lecture),” *Angewandte Chemie International Edition in English* **32**, 1111–1121 (1993).

[9] A. Nitzan, *Chemical Dynamics in Condensed Phases: Relaxation, Transfer, and Reactions in Condensed Molecular Systems*, Oxford Graduate Texts (OUP Oxford, 2013).

[10] Aurélia Chenu and Gregory D. Scholes, “Coherence in energy transfer and photosynthesis,” *Annual Review of Physical Chemistry* **66**, 69–96 (2015).

[11] S. Kais, K.B. Whaley, A.R. Dinner, and S.A. Rice, *Quantum Information and Computation for Chemistry*, Advances in Chemical Physics (Wiley, 2014).

[12] Paul E. Teichen and Joel D. Eaves, “A microscopic model of singlet fission,” *The Journal of Physical Chemistry B* **116**, 11473–11481 (2012).

[13] A.J. Leggett, S. Chakravarty, A.T. Dorsey, M.P.A. Fisher, A. Garg, and W. Zwerger, “Dynamics of the dissipative two-state system,” *Reviews of Modern Physics* **59**, 1–85 (1987).

[14] Alexandru Macridin, Panagiotis Spentzouris, James Amundson, and Roni Harnik, “Electron-phonon systems on a universal quantum computer,” *Phys. Rev. Lett.* **121**, 110504 (2018).

[15] Sabine Tornow, Ralf Bulla, Frithjof B. Anders, and Abraham Nitzan, “Dissipative two-electron transfer: A numerical renormalization group study,” *Phys. Rev. B* **78**, 035434 (2008).

[16] Dave Wecker, Matthew B. Hastings, Nathan Wiebe, Bryan K. Clark, Chetan Nayak, and Matthias Troyer, “Solving strongly correlated electron models on a quantum computer,” *Phys. Rev. A* **92**, 062318 (2015).

[17] R. Barends, L. Lamata, J. Kelly, L. García-Álvarez, A. G. Fowler, A. Megrant, E. Jeffrey, T. C. White, D. Sank, J. Y. Mutus, B. Campbell, Yu Chen, Z. Chen, B. Chiaro, A. Dunsworth, I. C. Hoi, C. Neill, P. J. J. O’Malley, C. Quintana, P. Roushan, A. Vainsencher, J. Wenner, E. Solano, and John M. Martinis, “Digital quantum simulation of fermionic models with a superconducting circuit,” *Nature Communications* **6**, 7654 (2015).

[18] Urtzi Las Heras, Laura García-Álvarez, Antonio Mezzacapo, Enrique Solano, and Lucas Lamata, “Fermionic models with superconducting circuits,” *EPJ Quantum Technology* **2**, 8 (2015).

[19] Ashley Montanaro and Stasja Stanisic, “Compressed variational quantum eigensolver for the fermi-hubbard model,” (2020), [arXiv:2006.01179 \[quant-ph\]](https://arxiv.org/abs/2006.01179).

[20] Guillermo García-Pérez, Matteo A. C. Rossi, and Sabrina Maniscalco, “Ibm q experience as a versatile experimental testbed for simulating open quantum systems,” *npj Quantum Information* **6**, 1 (2020).

[21] Lorenzo Del Re, Brian Rost, A. F. Kemper, and J. K. Freericks, “Driven-dissipative quantum mechanics on a lattice: Simulating a fermionic reservoir on a quantum computer,” *Phys. Rev. B* **102**, 125112 (2020).

[22] Martin Koppenhöfer, Christoph Bruder, and Alexandre Roulet, “Quantum synchronization on the ibm q system,” *Phys. Rev. Research* **2**, 023026 (2020).

[23] Zixuan Hu, Rongxin Xia, and Sabre Kais, “A quantum algorithm for evolving open quantum dynamics on quantum computing devices,” *Scientific Reports* **10**, 3301 (2020).

[24] Wibe A. de Jong, Mekena Metcalf, James Mulligan, Mateusz Płoskoń, Felix Ringer, and Xiaojun Yao, “Quantum simulation of open quantum systems in heavy-ion collisions,” (2020), [arXiv:2010.03571 \[hep-ph\]](https://arxiv.org/abs/2010.03571).

[25] Hefeng Wang, S. Ashhab, and Franco Nori, “Quantum algorithm for simulating the dynamics of an open quantum system,” *Phys. Rev. A* **83**, 062317 (2011).

[26] Bi-Xue Wang, Ming-Jie Tao, Qing Ai, Tao Xin, Neill Lambert, Dong Ruan, Yuan-Chung Cheng, Franco Nori, Fu-Guo Deng, and Gui-Lu Long, “Efficient quantum simulation of photosynthetic light harvesting,” *npj Quantum Information* **4**, 52 (2018).

[27] José Diogo Guimarães, Carlos Tavares, Luís Soares Barbosa, and Mikhail I. Vasilevskiy, “Simulation of nonradiative energy transfer in photosynthetic systems using a quantum computer,” *Complexity* **2020**, 1–12 (2020).

[28] H. De Raedt, F. Jin, M. I. Katsnelson, and K. Michielsen, “Relaxation, thermalization, and markovian dynamics of two spins coupled to a spin bath,” *Phys. Rev. E* **96**, 053306 (2017).

[29] Marco Cattaneo, Gabriele De Chiara, Sabrina Maniscalco, Roberta Zambrini, and Gian Luca Giorgi, “Collision models can efficiently simulate any multipartite markovian quantum dynamics,” (2020), [arXiv:2010.13910 \[quant-ph\]](https://arxiv.org/abs/2010.13910).

[30] James R. Wootton, “Benchmarking near-term devices with quantum error correction,” *Quantum Science and Technology* **5**, 044004 (2020).

[31] Richard Cleve and Chunhao Wang, “Efficient quantum algorithms for simulating lindblad evolution,” (2019), [arXiv:1612.09512 \[quant-ph\]](https://arxiv.org/abs/1612.09512).